Author Manuscript

Author Manuscript

Author Manuscript

Author Manuscript

HHS Public Access

Author manuscript

*J Magn Reson Imaging*. Author manuscript; available in PMC 2016 September 01.

Published in final edited form as:

*J Magn Reson Imaging*. 2015 September ; 42(3): 658–665. doi:10.1002/jmri.24825.

# Chronic fetal hypoxia affects axonal maturation in guinea pigs during development: a longitudinal Diffusion Tensor Imaging and $T_2$ mapping study

**Jieun Kim, PhD**[1], **In-Young Choi, PhD**[1,2,3], **Yafeng Dong, PhD**[4,5], **Wen-Tung Wang, PhD**[1], **William M. Brooks, PhD**[1,2], **Carl P. Weiner, MD**[2,4,5], and **Phil Lee, PhD**[1,2,*]

[1]Hoglund Brain Imaging Center, University of Kansas Medical Center, Kansas City, KS, USA

[2]The Department of Molecular & Integrative Physiology, University of Kansas Medical Center, Kansas City, KS, USA

[3]The Department of Neurology, University of Kansas Medical Center, Kansas City, KS, USA

[4]The Department of Obstetrics and Gynecology, University of Kansas Medical Center, Kansas City, KS, USA

[5]The Center for the Developmental Origins of Adult Health and Disease, University of Kansas Medical Center, Kansas City, KS, USA

## Abstract

**Purpose—**Chronic hypoxemia is the prime cause of fetal brain injury and long-term sequelae such as neurodevelopmental compromise, seizures and cerebral palsy. This study aims to investigate the impact of chronic hypoxemia on neonatal brains, and follow developmental alterations and adaptations non-invasively in a guinea pig model.

**Materials and Methods—**Thirty guinea pigs underwent either normoxic and hypoxemic conditions during the critical stage of brain development (0.7 gestation) and studied prenatally (n=16) or perinatally (n=14). Fourteen newborns (7 hypoxia and 7 normoxia group) were scanned longitudinally to characterize physiological and morphological alterations, and axonal myelination and injury using *in vivo* DTI, $T_2$ mapping, and $T_2$-weighted MRI. Sixteen fetuses (8 hypoxia and 8 normoxia) were studied *ex vivo* to assess hypoxia-induced neuronal injury/loss using Nissl staining and quantitative reverse transcriptase Polymerase Chain Reaction methods.

**Results—**Developmental brains in the hypoxia group showed lower fractional anisotropy in the corpus callosum (−12%, $p$=0.02) and lower $T_2$ values in the hippocampus (−16%, $p$=0.003) compared with the normoxia group with no differences in the cortex ($p$>0.07), indicating vulnerability of the hippocampus and cerebral white matter during early development. Fetal guinea pig brains with chronic hypoxia demonstrated an over-tenfold increase in expression levels of hypoxia index genes such as erythropoietin and HIF-1α, and an over 40% reduction in neuronal density, confirming prenatal brain damage.

[*]**Corresponding Author**, Phil Lee, Ph.D., Hoglund Brain Imaging Center, 3901 Rainbow Blvd, Mail Stop 1052, University of Kansas Medical Center, Kansas City, KS 66160, USA, Tel: 913 588 0454, Fax: 913 588 9071, plee2@kumc.edu.

Author Manuscript Author Manuscript Author Manuscript Author Manuscript

**Conclusion—***In vivo* MRI measurement, such as DTI and $T_2$ mapping, provides quantitative parameters to characterize neuro-developmental abnormalities and to monitor the impact of prenatal insult on the postnatal brain maturation of guinea pigs.

### Keywords

Fetal hypoxia; DTI; $T_2$; guinea pig; prenatal brain injury; brain development

## INTRODUCTION

The developing fetal brain is vulnerable to numerous misadventures that may cause functional and behavioral deficits later in life. Many infants who survive very preterm birth develop neuronal and motor developmental deficits including spastic motor deficits such as cerebral palsy (1, 2) or cognitive, behavioral, attentional and socialization deficits (3–5). Increasing evidence suggests that one factor underlying many forms of fetal brain injury and abnormal brain development is oxygen deprivation, whether it occurs acutely (e.g., umbilical cord occlusion) (6–9) or chronically (e.g., impaired placental function and chronic fetal hypoxia) (10–13). Fetal neuropathology reflects both the severity and duration of these intrauterine insults, and the gestational age of the fetus at the time of insults in humans and experimental animal models (13, 14).

Both acute and chronic fetal hypoxia are relatively common complications associated with neuro-developmental abnormalities (13). Over 40% of intrauterine fetal or perinatal deaths are related to placental vascular problems (10). Acute hypoxic insults such as ischemia-perfusion injury during the early- to mid-gestation, when neurogenesis and neural migration are at their peak, lead to a rapid reduction in oxygen delivery to the brain, death of cerebellar Purkinje cells, hippocampal pyramidal cells and cortical neurons, and a slowing of neural migration, e.g., in the hippocampus (13). Even a relatively brief period of fetal hypoxia can have a significant impact on the fetal brain. For example, death of susceptible neuronal populations in the cerebellum, hippocampus and cortex, and cerebral white matter damage in animal models have been reported (1, 15). However, the causes and timing of fetal hypoxia are usually unknown in individual cases. It is also unclear whether it is hypoxia alone or hypoxia in combination with other physiological changes that render the fetal brain vulnerable to damage. An improved understanding of the etiology of perinatal brain damage should allow the development of new strategies to intervene and reduce the burden of perinatal brain injury.

Guinea pigs are a good model for human pregnancy complications such as chronic fetal hypoxia (16), because unlike rodents, guinea pigs undergo substantial brain development prior to birth similar to humans, and also possess a similarity to humans in placental vascular structure and a relatively long gestation, allowing for intrauterine manipulations at specific developmental stages (17). Moreover, guinea pigs are amenable to postnatal behavioral and functional testing. Although guinea pig models have been used to study a variety of conditions because of their human similarities, the brain development of guinea pigs in health and disease is not well characterized. In a previous study, a guinea pig model of 14 days of chronic fetal hypoxia, beginning at 46 to 49 days of gestation, resulted in

Author Manuscript Author Manuscript Author Manuscript Author Manuscript

selective brain injury in the cortex, hippocampus and thalamic nuclei; shorter exposures or milder degrees of hypoxia introduced later in gestation were proven less reliable as fetal brain growth was not altered, though histological damage was observed (16, 18).

MR relaxation times (especially, $T_1$ and $T_2$), related to tissue structure and the biophysical environment of brain water, have been widely used to characterize microstructural changes of brain tissue in various physiological and pathological conditions including aging, Alzheimer disease, Parkinson's disease, and stroke. Diffusion tensor imaging (DTI) provides distinctive endogenous contrast for brain tissue delineation as well as information about myelination and axonal integrity (19, 20). DTI has also been used to demonstrate subtle abnormalities in stroke, multiple sclerosis, dyslexia and schizophrenia, as well as in developing brains of rodents and humans (21). Although these quantitative MR techniques provide insights into postnatal developmental changes in the brain after an acute episode of hypoxia, the effect of chronic fetal hypoxia on the newborn has not been described in guinea pigs to date. The purpose of this longitudinal study was to characterize the physiological and morphological effects of chronic fetal hypoxia on brain development in a well-established guinea pig model of intrauterine hypoxia using *in vivo* DTI, $T_2$ mapping and $T_2$-weighted MRI techniques.

## MATERIALS AND METHODS

### Animals

All animal care and procedures were performed according to the guidelines for the care and use of laboratory animals, and approved by the Institutional Animal Care and Use Committee (IACUC). Time-mated pregnant Hartley-Duncan guinea pigs (Charles River Laboratories International, Inc, Wilmington, MA) were housed in a Plexiglass chamber for 14 days with room air estimated to be 21% $O_2$ for the normoxia (NMX) group and with 10.5% $O_2$ for the hypoxia (HPX) group. Chronic fetal hypoxia was induced in guinea pigs during 13–21 days before birth (or 45–53 days of fetal life), which was at 46 – 49 days of gestation (about 0.7 gestation, term approximately 65 days), according to an established hypoxic model (18). A total of 14 newborn guinea pigs (7 HPX and 7 NMX; 2 males in each group) from four litters were used in the longitudinal MR study up to 6 weeks of age. Sixteen guinea pig fetuses (8 HPX and 8 NMX) were used to assess hypoxia induced neuronal injury and neuronal loss.

For MRI experiments, animals were anesthetized by a gas mixture (air:oxygen = 2:1, with 1 – 2% isoflurane) delivered through a nose cone. The core body temperature was monitored using a rectal temperature sensor (Cole-Palmer, Vernon Hills, Illinois) and maintained at 38 °C with a warm water circulation blanket. The respiratory rate and blood oxygen saturation were monitored using a respiration pillow (SA instruments, Stony Brook, NY) and a pulse oximeter (Nonin Medical, Plymouth, MN), respectively.

### MRI protocol

All MR experiments were performed on a 9.4 T MR system with a Varian INOVA console (Agilent Technologies, Santa Clara, CA). The system was equipped with a 12 cm gradient

Author Manuscript Author Manuscript Author Manuscript Author Manuscript

coil (40 G/cm, 250 μs; Magnex Scientific, Abingdon, UK). A custom-made quadrature surface radiofrequency coil was placed on top of the animal head to transmit and receive at 400 MHz. The RF coil consisted of two geometrically decoupled loops, each 18 mm in diameter. DTI measurements were performed using a standard mono-polar diffusion weighted spin echo sequence (FOV = 2.5 × 2.5 $cm^2$, matrix = 128 × 128, TR/TE = 1000/23 ms, and diffusion gradients were applied along 6 different orientations, b = 832 $s/mm^2$, NEX = 2, slice thickness = 1 mm, and total acquisition time ~30 minutes). MRI of $T_2$ mapping was acquired using a multi-slice spin echo sequence: FOV = 2.5 × 2.5 $cm^2$, matrix = 128 × 128, TR = 1 s, TE = 12/24/36/48/60 ms, NEX = 2, slice thickness = 1 mm and total acquisition time =~20 minutes (~4 minutes for each TE). Both DTI and $T_2$ MRI were acquired in identical slice positions, FOV and spatial resolution. High-resolution $T_2$-weighted images were acquired to quantify brain volume and to define regions of interest using a rapid acquisition with relaxation enhancement (RARE) sequence (FOV = 3.0 × 3.0 $cm^2$, matrix = 256 × 256, TR/TE = 4000/72 ms, NEX = 2, thickness = 1 mm, echo train length = 8, echo spacing = 18 ms and total acquisition time ~4 minutes). $T_2$-weighted MRI, $T_2$ mapping and spin-echo DTI data were acquired at four time-points, postnatal day 1 (P1), 7 (P7), 28 (P28) and 42 (P42), from the 14 neonatal guinea pigs (7 HPX and 7 NMX), and the body weight was measured at 5 time-points: P1, P7, P14, P28 and P42.

## Data analysis

Spin-echo DTI data were processed using the FSL diffusion toolbox (FDT) (22) with manually segmented brain masks, and parametric maps of fractional anisotropy (FA), mean diffusivity (MD), and axial and radial diffusivity were generated. The eddy current correction on DTI data was not necessary, because a non-EPI based SE sequence with very short readout duration, 2.5 ms, was used, and eddy currents were minimal due to the relatively low diffusion gradient amplitude (less than 40% of the maximum). $T_2$ maps were calculated using linear fitting of the logarithm of each pixel value against TE values using ImageJ (23). Regional values for diffusion parameters (FA, MD and axial and radial diffusivity) were obtained from the regions of interest (ROI) placed in the corpus callosum, hippocampus, cortex and cingulate (Fig 2a). Regional $T_2$ values were obtained from the ROIs placed in the hippocampus and cortex (Fig. 2a). ROIs for $T_2$ maps and DTI parameters (except FA in the corpus callosum) were drawn over low resolution, long TE (60 ms) $T_2$-weighted MRI. ROIs for FA in the corpus callosum were drawn on the FA maps (Fig. 2b), which provide the best contrast of the corpus callosum to the background. Care was taken in drawing each ROI to prevent inclusion of areas surrounding the corpus callosum.

Brain structural changes were quantified by measuring the maximum brain width, mean cortical thickness and hippocampal volume using high resolution $T_2$-weighted MRI (Fig. 2a). Maximum brain width was measured at the widest part of the brain (Fig.2a, left). Mean cortical thickness was obtained by measuring the shortest distances between the corpus callosum and the outer brain surface at the locations in both hemispheres (Fig. 2a, right). Hippocampal volume was obtained by summing pixel volumes in the ROIs drawn over three or four consecutive slices of high resolution $T_2$-weighted MRI.

Author Manuscript Author Manuscript Author Manuscript Author Manuscript

### Neuron loss identification by Nissl staining

Fetal brains from both groups were removed intact and fixed in 4% paraformaldehyde overnight at 4 °C, cryoprotected in 30% sucrose for 2–3 days at 4 °C until no longer buoyant, and then embedded in OCT frozen tissue matrix for sectioning. Coronal sections were made at the interaural level of 6.72 mm to 5.40 mm (reference to bregma: from −2.28 mm to −3.60 mm) of the fetal brain, and cut on a cryostat (−20 °C) at 8 μm thickness and mounted on slides.

The slides were used to quantify neuronal density using Nissl staining with Cresyl violet. Frozen slides were air dried for 1 hour, stained in Cresyl violet solution (0.1 % Cresyl violet) for 5 minutes, rinsed in distilled water, differentiated in 95% ethyl alcohol for 15 minutes, dehydrated in 100% alcohol for 5 minutes twice, cleared in xylene for 5 minutes twice, and then mounted by resinous medium for the quantification. Each stained section was examined by a research team member (YD) with over 10 years' experience using light microscopy, and neuron density in the fetal brain was quantified as previously reported (18).

### Quantitative reverse transcriptase polymerase chain reaction (qRT-PCR)

Hypoxia index genes (EPO and HIF1a) were used as fetal brain injury markers. mRNA expression was quantified by SYBR Green I (BioRad Laboratories, Hercules, CA) labeled quantitative real time Polymerase Chain Reaction (qRT-PCR) using mRNA extracted from specific brain structures using laser biopsies. Total RNA was isolated (RNeasy Mini Kit and RNase-Free DNase Set, Qiagen, Valencia, CA) and reverse-transcribed (Sensiscript RT Kits, Qiagen, Valencia, CA). The primer sequence for each gene target was performed by Beacon Designer 5.0 (BioRad Laboratories, Hercules, CA) using procedures described previously (24, 25). PCR parameters consisted of an initial denaturation at 95 °C for 180 seconds, followed by 40 cycles at 95 °C for 30 seconds, annealing at 60 °C for 25 seconds, extension at 72 °C for 30 seconds, and 1 cycle at 72 °C for 7 minutes. The results of a melt analysis confirmed the specificity of the PCR amplification. PCR efficiency was demonstrated by the standard curve slope. Target gene mRNA was quantified by the delta-delta CT (2-DDCt) method and normalized to the 18S subunit of rRNA (Applied Biosystems, Foster City, CA).

### Statistical analysis

All measurement parameters including FA, MD, axial diffusivity, radial diffusivity, hippocampal volume, brain width, cortical thickness, and body weight for the HPX and NMX groups were compared using two-sample t-tests. Longitudinal comparisons were performed using one-sample t-test. Results are presented as mean ± standard deviation (SD). Differences between or within groups with p-values less than 0.05 were considered to be statistically significant.

## RESULTS

### Histological and biochemical characterization of hypoxia model

Photomicrographs of hippocampal sections with Nissl staining show a clear reduction of the total areas with the staining in the HPX group (Fig. 1A right) compared with the NMX

Author Manuscript Author Manuscript Author Manuscript Author Manuscript

group (Fig. 1A left). Neuronal density quantified using the Nissl stained sections showed a more than 40% reduction ($p < 0.05$) in all three sampled brain regions of the HPX group compared with the NMX group (Fig. 1B). The mRNA expression levels of two injury markers, erythropoietin (EPO) and HIF-1α, showed over 10-fold elevation ($p < 0.05$) in the HPX group compared with the NMX group (Fig. 1C).

### DTI measurements

FA values in the corpus callosum showed gradual increases during postnatal brain development from P1 to P42 in both NMX and HPX groups (Fig. 3a). The HPX group showed significantly lower FA values in the corpus callosum than NMX group shortly after birth to P7 (P1:−10%, $p < 0.05$; P7: −12%, $p < 0.02$). FA values in the hippocampus, cingulate or cortex showed no detectable developmental changes or group differences ($p > 0.07$). MD values in the corpus callosum (Fig. 3b) and other areas such as the hippocampus, cortex and cingulate (data not shown), showed no detectable changes with advancing postnatal ages or group differences ($p > 0.07$). Similar to MD, axial diffusivity and radial diffusivity in the corpus callosum showed no age dependency or group differences ($p > 0.08$).

### $T_2$ measurements

$T_2$ values showed no longitudinal changes in the hippocampus and cortex of both groups during the first 42 days of life (Fig. 4). However, $T_2$ values in hippocampal regions were significantly lower in the HPX group compared with those in the NMX group, particularly at P7 ($p < 0.01$) and P28 ($p < 0.02$) (Fig. 4a), while the difference at P1 did not reach statistical significance ($p = 0.17$). $T_2$ values in the cortex did not differ between groups ($p > 0.08$) (Fig. 4b).

### Brain structural measurements

Body weight (Fig. 5a) increased rapidly more than threefold after birth during the 42 day period for both groups. Brain width and hippocampal volume increased steadily from P1 to P42 in both groups over 11% and 15%, respectively. Brain width and hippocampal volume showed similar patterns of changes for both groups over the first 42 days of post-natal life, an initial rapid increase followed by a slower increase (Fig. 5b and 5c). Although statistically not significant, overall brain width and hippocampal volume were consistently smaller in the HPX group compared with those in the NMX group. In contrast, cortical thickness did not change with advancing postnatal age, nor showed any difference between the HPX and NMX groups (Fig. 5d).

## DISCUSSION

Quantitative $T_2$ mapping and DTI techniques allow us to detect subtle yet significant changes of brain morphology and microstructure in a guinea pig model of chronic fetal hypoxia. This study describes the first in vivo characterization of brain development and the effect of fetal hypoxia, i.e., reduced $T_2$ in the hippocampus and lower FA in corpus callosum, particularly in guinea pigs. Chronic fetal hypoxia during the major brain growth period resulted in decreased neuronal density and increased activation of hypoxia index

Author Manuscript Author Manuscript Author Manuscript Author Manuscript

gene, corroborating the association between chronic hypoxia and fetal brain injury. Our data are consistent with previous findings of the effect of chronic hypoxia resulting in intrauterine growth restriction and neuronal loss in animal models, as well as findings in human fetuses with chronic hypoxia (26, 27). Furthermore, our data are consistent with previous studies of chronic hypoxia in fetal sheep showing significant delays in cell migration from the germinal to the pyramidal layers of the CA1 region in the ventral hippocampus and decreases of pyramidal neuron density by 35% (28).

Increases of FA values over time in the corpus callosum in both NMX and HPX groups are consistent with various processes occurring during brain development, which includes axonal myelination, decreased axonal tortuosity, removal of cell membranes along the longitudinal axis of axons, and increased axonal density or caliber (21,29–34). The finding of lower FA values in the corpus callosum of the HPX group compared with the NMX group suggests chronic fetal hypoxia delays myelination and white matter maturation as FA describes the degree of molecular displacement variability in space (ellipsoid eccentricity) and is related to the presence of oriented structures such as axons in white matter. Although the FA values in the corpus callosum of the HPX group gradually increased over time, overall FA values remained lower in the HPX group than those of the NMX group. The delayed myelination, white matter maturation and/or potential injury during the early developmental phase of the HPX group seems to diminish during postnatal development as the differences of FA values decrease overtime between the two groups.

Prior studies of the developing brain reported longer $T_2$ values in young animals and gradual decreases of $T_2$ values during brain maturation. In the mouse brain, this initial rapid decrease in $T_2$ values occurs during the first 3 weeks (21). However, we observed no significant changes of $T_2$ values during the first several weeks after birth, up to 6 weeks, in the hippocampus and cortex, which is not surprising because brain growth spurt of guinea pigs occurs in utero during the third trimester and brain weight reaches over 80% of adult brain weight in utero unlike any other animals (35). Lower hippocampal $T_2$ values in the HPX group compared with the NMX group suggest fetal hypoxia alters postnatal brain maturation. $T_2$ values in the hippocampus at P28 were still significantly lower in the HPX group than the NMX group, and remained lower at P42. Studies at later ages are needed to determine whether the lower $T_2$ in the HPX group can be recovered as the brain further matures. Reductions of $T_2$ values in the brain have been associated with decreased cerebral blood flow in rats (36), iron deposition in humans (37), and iron deposition that co-localizes with beta-amyloid plaque deposition in transgenic mouse models of Alzheimer disease (38, 39). Considering very low levels of non-heme iron levels in the neonatal brains, the effect of iron might not be a significant factor for the observed $T_2$ reduction, but rather the effect of lower cerebral blood flow might be more likely the cause of the $T_2$ reduction because loss of neurons and brain atrophy have been associated with reduced cerebral blood flow in various pathological conditions including neurodegenerative diseases (40).

This study provides quantitative measurements of the effects of chronic fetal hypoxia on brain structure such as hippocampal volume, brain width and cortical thickness during brain development of guinea pig neonates from birth to young adulthood. The hippocampal volumes in HPX were consistently smaller than those in the NMX group. These findings are

Author Manuscript Author Manuscript Author Manuscript Author Manuscript

consistent with the demonstration of significant neuronal loss and reactive gliosis in those areas of the guinea pig neonates in this study as well as in previous findings (18).

A limitation of this study is that analysis of other brain structures such as the striatum was not feasible due to the use of a surface coil to increase the sensitivity of MR measurement. A whole brain acquisition strategy with a volume coil could help to assess the global effects of chronic fetal hypoxia. Another limitation of this study is a lack of histological analyses at various time points during the brain development of guinea pigs to compare with our MRI findings. Further study will be necessary to determine functional consequences of early brain abnormalities observed in both MRI and histology analyses, and to confirm the degree of apparent brain recovery during development and in later life through the long-term assessment of histology and histochemical markers in animal models.

In conclusion, *in vivo* DTI and $T_2$ mapping can provide parameters to monitor developmental abnormalities of neonates from birth to postnatal development in a totally noninvasive and longitudinal manner. Non-invasive neuroimaging measurements of pathophysiological and structural alterations during postnatal development may provide insight into the status of brain damage, neurodevelopmental compromise and long-term consequences of intrauterine insults.

## Acknowledgements

**Grant Support:**

This study was supported by the Public Health Service (R01 HL049041-13; CPW), Centers for Disease Control and Prevention (DP00187-5; CPW), and the National Institute of Child Health and Human Development (RO3 HD062734; YD). The Hoglund Brain Imaging Center is supported by a generous gift from Forrest and Sally Hoglund and funding from the National Institutes of Health (P30 HD002528, S10 RR29577, UL1 RR033179, and P30 AG035982).

## References

1. Holling EE, Leviton A. Characteristics of cranial ultrasound white-matter echolucencies that predict disability: a review. Dev Med Child Neurol. 1999; 41:136–139. [PubMed: 10075101]
2. Platt MJ, Cans C, Johnson A, et al. Trends in cerebral palsy among infants of very low birthweight (<1500g) or born prematurely (<32 weeks) in 16 European centres: a database study. Lancet. 2007; 369:43–50. [PubMed: 17208641]
3. Allin M, Walshe M, Fern A, et al. Cognitive maturation in preterm and term born adolescents. J Neurol Neurosurg Psychiatr. 2008; 79:381–386. [PubMed: 17682017]
4. Larroque B, Ancel P-Y, Marret S, et al. Neurodevelopmental disabilities and special care of 5-year-old children born before 33 weeks of gestation (the EPIPAGE study): a longitudinal cohort study. Lancet. 2008; 371:813–820. [PubMed: 18328928]
5. Woodward LJ, Edgin JO, Thompson D, Inder TE. Object working memory deficits predicted by early brain injury and development in the preterm infant. Brain. 2005; 128:2578–2587. [PubMed: 16150850]
6. Bejar R, Wozniak P, Allard M, et al. Antenatal origin of neurologic damage in newborn infants. I. Preterm infants. American journal of obstetrics and gynecology. 1988; 159(2):357–363. [PubMed: 3407693]
7. Nelson KB, Leviton A. How much of neonatal encephalopathy is due to birth asphyxia? American journal of diseases of children. 1991; 145(11):1325–1331. [PubMed: 1835281]
8. du Plessis AJ, Volpe JJ. Perinatal brain injury in the preterm and term newborn. Current opinion in neurology. 2002; 15(2):151–157. [PubMed: 11923628]

Author Manuscript Author Manuscript Author Manuscript Author Manuscript


9. Shankaran S, Laptook AR, Ehrenkranz RA, Tyson JE, McDonald SA, Donovan EF. Whole-body hypothermia for neonates with hypoxic-ischemic encephalopathy. N Eng J Med. 2005; 353:1574–1584.
10. Grafe MR. The correlation of prenatal brain damage with placental pathology. J Neuropathol Exp Neurol. 1994; 53:407–415. [PubMed: 8021715]
11. Salihagic-Kadic A, Medic M, Jugovic D, et al. Fetal cerebrovascular response to chronic hypoxia--implications for the prevention of brain damage. The journal of maternal-fetal & neonatal medicine : the official journal of the European Association of Perinatal Medicine, the Federation of Asia and Oceania Perinatal Societies, the International Society of Perinatal Obstet. 2006; 19(7): 387–396.
12. Rees S, Harding R, Walker D. An adverse intrauterine environment: implications for injury and altered development of the brain. International journal of developmental neuroscience : the official journal of the International Society for Developmental Neuroscience. 2008; 26(1):3–11. [PubMed: 17981423]
13. Rees S, Harding R, Walker D. The biological basis of injury and neuroprotection in the fetal and neonatal brain. Int J Dev Neurosci. 2011; 29(6):551–563. [PubMed: 21527338]
14. Baschat, AA. Fetal Growth Abnormalities. In: James, D.; Steer, P.; Weiner, CP.; Gonik, B.; Crowther, C.; Robson, S., editors. High Risk Pregnancy: Management Options. Philadelphia: Elsevier; 2011. p. 173-192.
15. Gunn AJ, Bennet L. Fetal hypoxia insults and patterns of brain injury: insights from animal models. Clin Perinatol. 2009; 36:579–593. [PubMed: 19732615]
16. Thompson LP, Aguan K, Pinkas G, Weiner CP. Chronic hypoxia increases the NO contribution of acetylcholine vasodilation of the fetal guinea pig heart. Am J Physiol Regulatory Integrative Comp Physiol. 2000; 279:R1813–R1820.
17. Pappas JJ, Petropoulos S, Suderman M, et al. The multidrug resistance 1 gene abcb1 in brain and placenta: comparative analysis in human and Guinea pig. PloS one. 2014; 9(10):e111135. [PubMed: 25353162]
18. Dong Y, Yu Z, Sun Y, et al. Chronic fetal hypoxia produces selective brain injury associated with altered nitric oxide synthases. Am J Obstet Gynecol. 2011; 204:254, e216–e228. [PubMed: 21272843]
19. Zhang J, Miller MI, Plachez C, et al. Mapping postnatal mouse brain development with diffusion tensor microimaging. NeuroImage. 2005; 26:1042–1051. [PubMed: 15961044]
20. Wozniak JR, Lim KO. Advances in white matter imaging: A review of in vivo magnetic resonance methodologies and their applicability to the study of development and aging. Neurosci & Biobehav Rev. 2006; 30:762–774. [PubMed: 16890990]
21. Mori S, Zhang J. Principles of Diffusion Tensor Imaging and Its Applications to Basic Neuroscience Research. Neuron. 2006; 51:527–539. [PubMed: 16950152]
22. Smith SM, Jenkinson M, Woolrich MW, et al. Advances in functional and structural MR image analysis and implementation as FSL. NeuroImage. 2004; 23:S208–S219. [PubMed: 15501092]
23. Rasband, WS. ImageJ. Bethesda, MD, USA: National Institute of Health; 1997–2011. p. http://imagej.nih.gov/ij/.
24. Hagstrom L, Agbulut O, El-Hasnaoui-Saadani R, et al. Epo is relevant neither for microvascular formation nor for the new formation and maintenance of mice skeletal muscle fibres in both normoxia and hypoxia. J Biomed Biotechnol. 2010; 2010:137817. [PubMed: 20414335]
25. Toussaint M, Fievez L, Desmet CJ, et al. Increased hypoxia-inducible factor 1alpha expression in lung cells of horses with recurrent airway obstruction. BMC Vet Res. 2012; 8:64. [PubMed: 22621400]
26. Barrett RD, Bennet L, Davidson J, et al. Destruction and reconstruction: hypoxia and the developing brain. Birth defects research Part C, Embryo today : reviews. 2007; 81(3):163–176.
27. Guo R, Hou W, Dong Y, Yu Z, Stites J, Weiner CP. Brain injury caused by chronic fetal hypoxemia is mediated by inflammatory cascade activation. Reproductive sciences. 2010; 17(6): 540–548. [PubMed: 20360591]

Author Manuscript Author Manuscript Author Manuscript Author Manuscript


28. Rees S, Harding R. The effects of intrauterine growth retardation on the development of the Purkinje cell dendritic tree in the cerebellar cortex of fetal sheep: a not on the ontogeny of the Purkinje cell. Int J Dev Neurosci. 1988; 6:461–469. [PubMed: 2462330]
29. Neil JJ, Shiran SI, McKinstry RC, et al. Normal brain in human newborns: apparent diffusion coefficient and diffusion anisotropy measured by using diffusion tensor MR imaging. Radiology. 1998; 209:57–66. [PubMed: 9769812]
30. Huppi PS, Maiser SE, Peled S, et al. Microstructural Development of Human Newborn Cerebral White Matter Assessed in Vivo by Diffusion Tensor Magnetic Resonance Imaging. Pediatr Res. 1998; 44:584–590. [PubMed: 9773850]
31. Takahashi M, Ono J, Harada K, Maeda M, Hackney DB. Diffusional anisotropy in cranial nerves with maturation: quantitative evaluation with diffusion MR imaging in rats. Radiology. 2000; 216(3):881–885. [PubMed: 10966726]
32. Provenzale JM, Isaacson J, Chen S, Stinnett S, Liu C. Correlation of apparent diffusion coefficient and fractional anisotropy values in the developing infant brain. AJR Am J Roentgenol. 2010; 195(6):W456–W462. [PubMed: 21098179]
33. Baratti C, Barnett AS, Pierpaoli C. Comparative MR Imaging Study of Brain Maturation in Kittens with T1, T2, and the Trace of the Diffusion Tensor. Radiology. 1999; 210:133–142. [PubMed: 9885598]
34. Wang S, Wu EX, Tam CN, Lau H-F, Cheung P-T, Khong P-L. Characterization of White Matter Injury in a Hypoxic-Ischemic Neonatal Rat Model by Diffusion Tensor MRI. Stroke. 2008; 39:2348–2353. [PubMed: 18535275]
35. Dobbing J, Sands J. Growth and development of the brain and spinal cord of the guinea pig. Brain Res. 1970; 17(1):115–123. [PubMed: 5412929]
36. Grohn OH, Kettunen MI, Penttonen M, Oja JM, van Zijl PC, Kauppinen RA. Graded reduction of cerebral blood flow in rat as detected by the nuclear magnetic resonance relaxation time T2: a theoretical and experimental approach. J Cereb Blood Flow Metab. 2000; 20(2):316–326. [PubMed: 10698069]
37. Bartzokis G, Sultzer D, Cummings J, et al. In vivo evaluation of brain iron in Alzheimer disease using magnetic resonance imaging. Arch Gen Psychiatry. 2000; 57(1):47–53. [PubMed: 10632232]
38. Helpern JA, Lee SP, Falangola MF, et al. MRI assessment of neuropathology in a transgenic mouse model of Alzheimer's disease. Magnetic resonance in medicine : official journal of the Society of Magnetic Resonance in Medicine / Society of Magnetic Resonance in Medicine. 2004; 51(4):794–798.
39. Lee SP, Falangola MF, Nixon RA, Duff K, Helpern JA. Visualization of beta-amyloid plaques in a transgenic mouse model of Alzheimer's disease using MR microscopy without contrast reagents. Magnetic resonance in medicine : official journal of the Society of Magnetic Resonance in Medicine / Society of Magnetic Resonance in Medicine. 2004; 52(3):538–544.
40. Schuff N, Matsumoto S, Kmiecik J, et al. Cerebral blood flow in ischemic vascular dementia and Alzheimer's disease, measured by arterial spin-labeling magnetic resonance imaging. Alzheimers Dement. 2009; 5(6):454–462. [PubMed: 19896584]

Author Manuscript Author Manuscript Author Manuscript Author Manuscript

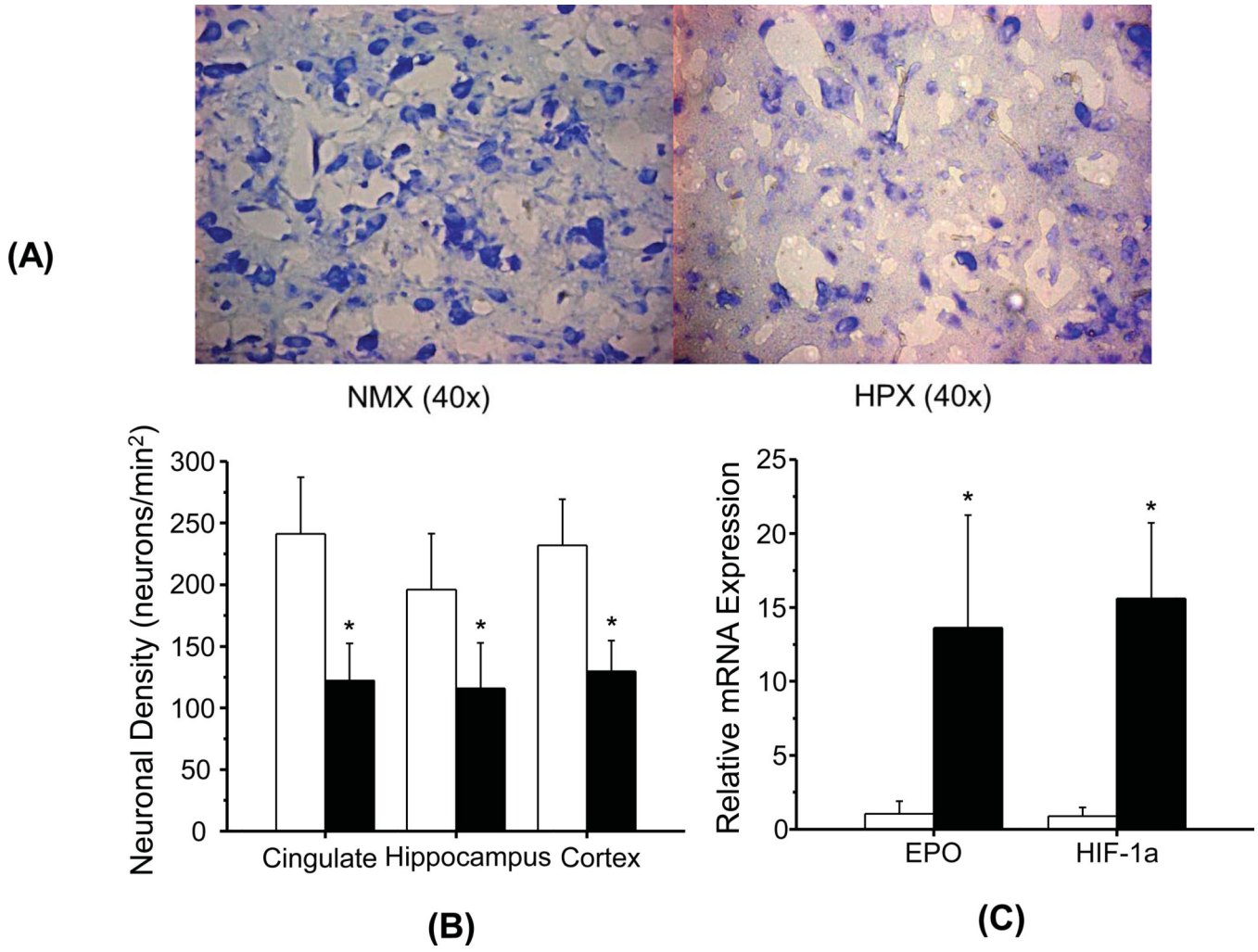


**Figure 1.**

Effect of chronic fetal hypoxia on neuronal density and brain injury markers in the fetal brain. Photomicrographs of Nissle stained coronal sections of the fetal guinea pig brains in the NMX (a, left) and HPX (a, right) groups at the interaural level of 6.72–5.40 mm. Neuronal structures with RNA are shown in blue. (b) Neuronal density in cingulate, hippocampus, and cortex. Neuronal density was measured from histological sections of each region by counting the number of Nissl stained cells per square millimeter. (c) Expression levels of mRNA for brain injury indices (EPO and H1F-1α) in hippocampus. (*) indicates significant differences ($p < 0.05$) between the HPX and NMX groups.

Author Manuscript Author Manuscript Author Manuscript Author Manuscript

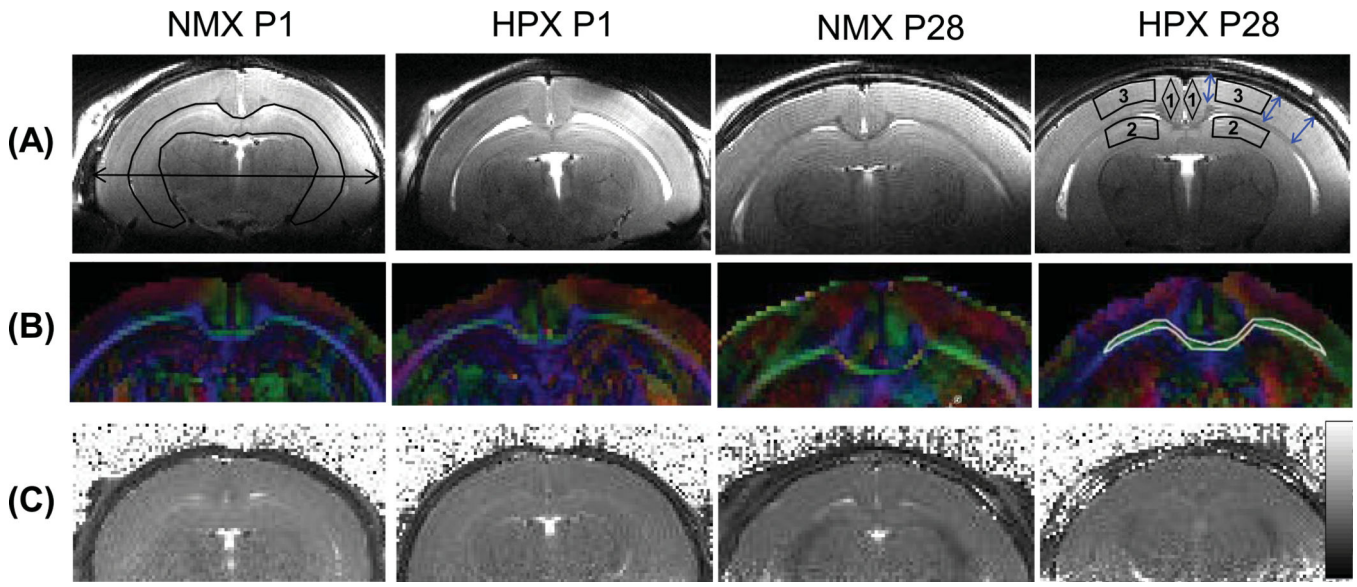


**Figure 2.**

MR images of guinea pig brains in the NMX and HPX groups at postnatal day 1 (P1) and 28 (P28). (a) High resolution $T_2$-weighted images during brain development of guinea pigs. The ROI of the hippocampus and a double-headed arrow indicating maximum brain width measurements are shown in the NMX P1 image (top, leftmost). The ROIs for $T_2$ sampling are shown in the 'HPX P28' image: 1) cingulate, 2) hippocampus and 3) cortex, and three double-headed blue arrows indicate areas where cortical thickness was measured. (b) RGB fractional anisotropy (FA) maps corresponding to high resolution $T_2$-weighted images in (a). An ROI of the corpus callosum is shown in the P28 HPX image (middle, rightmost). Colors indicate different diffusion directions: red for x (left to right), green for y (caudal-rostral) and blue for z (anterior-posterior). (c) Corresponding $T_2$ maps at P1 and P28 of a normoxic and a hypoxic brains. The gray scale bar on the right indicates $T_2$ values between 10–100 ms.

Author Manuscript Author Manuscript Author Manuscript Author Manuscript

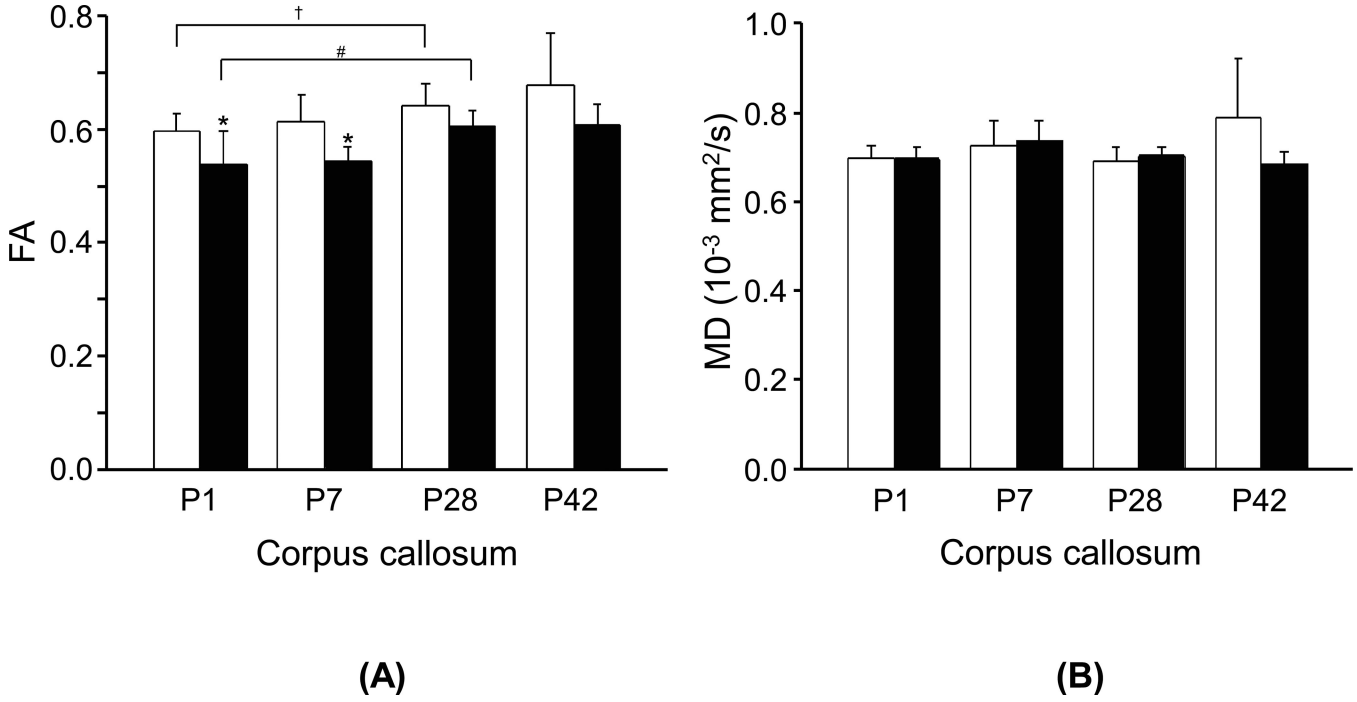


**(A)** **(B)**

**Figure 3.**

Comparisons of (a) FA and (b) MD values from the corpus callosum of guinea pig brains between the NMX (□) and HPX (■) groups at postnatal days 1 (P1), 7 (P7), 28 (P28) and 42 (P42). (*) indicates significant differences ($p < 0.05$) between the HPX and NMX groups at each age. (#) and (†) indicate significant longitudinal differences ($p < 0.05$) between P1 and P28 in the HPX and NMX groups, respectively.

Author Manuscript Author Manuscript Author Manuscript Author Manuscript

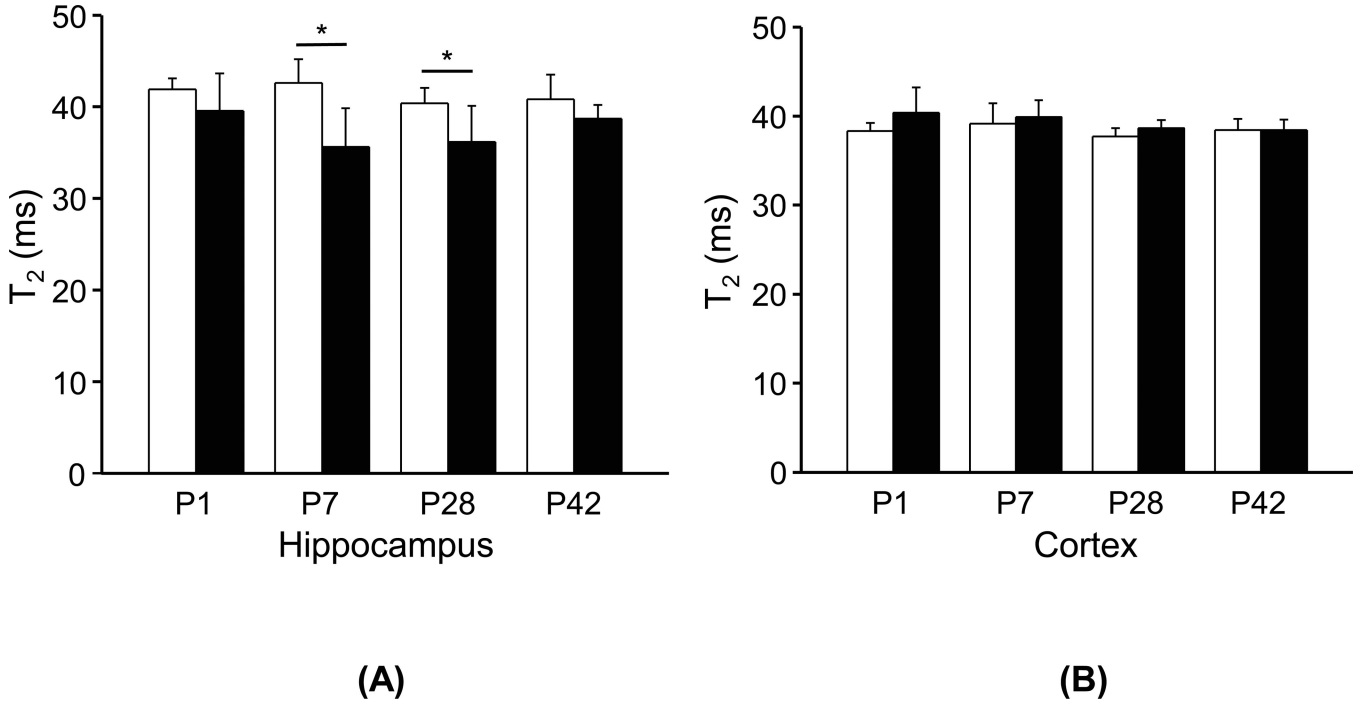


**Figure 4.**

Comparisons of $T_2$ values in (a) the hippocampus and (b) the cortex of guinea pigs brains between the NMX (□) and HPX (■) groups at postnatal days 1 (P1), 7 (P7), 28 (P28) and 42 (P42). (*) indicates significant differences ($p < 0.05$) between the HPX and NMX groups at each age.

Author Manuscript Author Manuscript Author Manuscript Author Manuscript

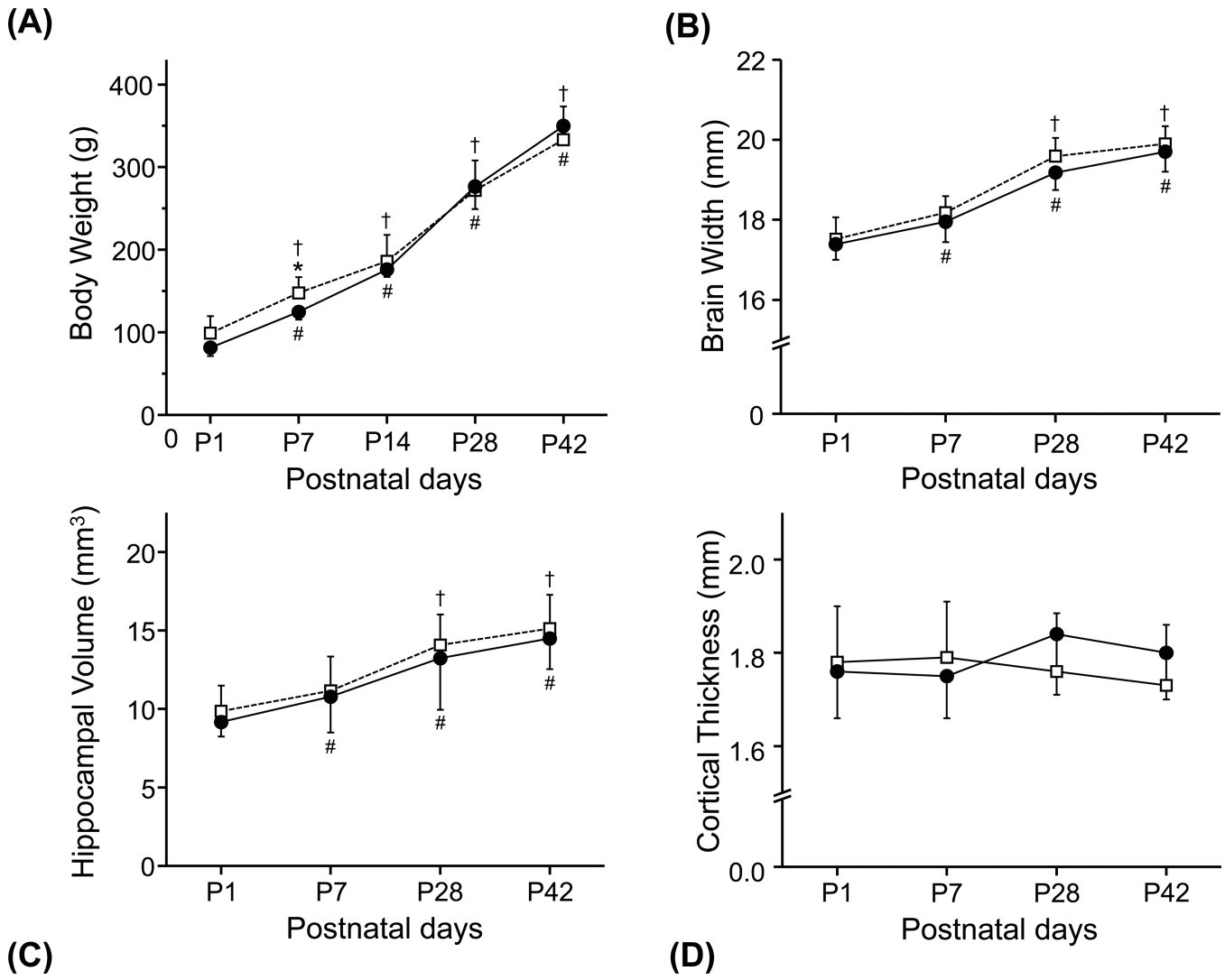


**Figure 5.**

Comparisons of structural changes of guinea pig brains in the NMX (□) and HPX (■) groups at postnatal days 1 (P1), 7 (P7), 28 (P28) and 42 (P42). Time course of (a) body weight, (b) brain width, (c) hippocampal size and (d) cortical thickness are shown from P1 to P42. (*) indicates significant differences ($p < 0.05$) between the HPX and NMX groups at each age. (#) and (†) indicate significant longitudinal differences ($p < 0.05$) between P1 and P7 to P28 in the HPX and NMX groups, respectively.